Tropical cyclones intensify mesoscale eddy variability and accelerate Western Boundary Current instability

Yongfei Deng[1], Tianning Wu[1], Scott Glenn[2], Ruoying He[1,*]

[1]Department of Marine, Earth, and Atmospheric Sciences, North Carolina State University, Raleigh, North Carolina, U.S. A.

[2]Department of Marine and Coastal Sciences, Rutgers University, New Brunswick, New Jersey, USA

Corresponding author: *rhe@ncsu.edu

Abstract

Tropical cyclones strongly disrupt the upper ocean, yet their influence on mesoscale variability in western boundary current systems remains poorly quantified. The Gulf of Mexico, where the Loop Current regularly sheds large warm-core eddies, offers an ideal setting to examine how hurricanes reshape mesoscale dynamics. Using a high-resolution ocean model and hurricane-denial experiments, we analyze the 2024 passage of Hurricanes Helene and Milton and their impacts on the Loop Current Eddy (LC/LCE) mesoscale variability. Hurricane Helene generated pronounced surface cooling by ~0.3°C, weakened the Loop Current, and strengthened the Tortugas cyclonic eddy (CE). Hurricane Milton further enhanced these anomalies and coincided with the detachment of LCE Edison. The combined effect of the two storms was nonlinear: Helene's cold wake and eddy intensification preconditioned the response to Milton and accelerated eddy separation. Here we show that sequential tropical cyclones can amplify cyclonic vorticity by up to 28%, enhance baroclinic instability through upwelling within the CE, and help boost the LCE shedding by ~6 days earlier, with important implications under a warming climate with more intense storms.

Introduction

Western boundary currents (WBCs) such as the Gulf Stream, Kuroshio, and Loop Current (LC) are dynamically active systems that transport heat, salt, and momentum poleward and strongly influence regional climate and weather[1–5]. In the Gulf of Mexico (GoM), the LC intrudes northward through the Yucatán Channel and periodically sheds large warm-core Loop Current Eddies (LCEs) that drift westward[6–8], while cyclonic eddies (CEs) frequently form along the LC's northern boundary, propagate southward along the eastern boundary, and stall near the Dry Tortugas region[9–12]. This LC–eddy complex sets the stage for strong mesoscale variability and has major consequences for shipping, offshore energy infrastructure, and hurricane intensification.

Tropical cyclones (TCs) are intense, rapidly evolving air–sea coupled systems[13]. Their atmospheric dynamics, boundary-layer structure, and sensitivity to sea-surface temperature (SST) and subsurface stratification have been extensively studied using theory, observations, and numerical models[14–16] . Recent work has highlighted global increases in TC intensification rates and rapid intensification events[17,18] and the critical role of GoM conditions in the intensification of storms such as Michael[19] and Ian[20]. However, much of this work has focused on the atmosphere and air–sea fluxes rather than the ocean's mesoscale eddy field and its subsurface variability.

The deep-water upper-ocean response to TCs is characterized by inertial currents, strong upwelling, turbulent mixing, and entrainment of colder, nutrient-rich waters from below the mixed layer, leading to pronounced cold wakes and changes in stratification[21–29]. Classical studies showed that wind-driven mixing beneath hurricanes can cool the surface by several degrees, with the magnitude and structure of the response depending sensitively on pre-existing stratification and mixed-layer depth [21,22]. Regional case studies in the GoM and western Pacific have linked such responses to changes in SST, biogeochemistry, and boundary-layer enthalpy fluxes [23–25] . Recent SWOT altimetry observations of Hurricane Idalia revealed multiple cold-core cyclonic eddies on the West Florida shelf whose cool surface temperatures likely suppressed storm intensification [30]. While the influence of pre-existing eddies and warm rings on hurricane evolution is now well recognized [30–32], the reverse process—how hurricanes reshape the eddy field and the stability of WBC systems—has received much less attention.

Studies in both the Atlantic and Pacific suggest that TCs can inject cyclonic vorticity, intensify CEs, generate new eddies, and disrupt anticyclonic rings [25,32,33]. Yet a quantitative assessment of how sequential TCs modulate LC structure, alter baroclinic instability, and accelerate LCE shedding has been lacking. This gap is particularly important given projections of climate change. Anthropogenic warming is expected to increase upper-ocean heat content and the likelihood of rapid intensification and very intense storms, even if changes in overall TC frequency remain uncertain [17,18,34–36]. These changes imply that storm–eddy interactions could

become more frequent and energetic, with potential feedbacks on WBC variability and coastal hazards.

The GoM is ideally suited to address these questions because it lies at the intersection of a vigorous LC system and recurrent TC pathways. Over the last 5 years, major hurricanes Ida, Ian, Idalia, Helene and Milton all crossed over the eastern Gulf's Loop Current system on their way to northeastern Gulf landfall. In 2024, Hurricanes Helene and Milton formed in the western Caribbean and central GoM, respectively, both made landfall in Florida within 2 weeks of each other, and generated extreme coastal water-level anomalies [37]. Their tracks intersected a dynamically active LC configuration in which a large warm-core eddy was attached to the LC and a Tortugas CE was present. Here we use a high-resolution regional ocean model, configured as an adaptation of the Coupled Northwest Atlantic Prediction System 2.0 (CNAPS2[38]), together with a couple of atmospheric feature-denial experiments, where we look at the sensitivity of the ocean to presence or absence of specific atmospheric structures, to quantify how Helene and Milton modified (i) upper-ocean thermal and current structures, (ii) the Tortugas CE, and (iii) the timing and structure of LCE Edison detachment. We show that sequential TCs can act as powerful amplifiers of mesoscale variability and LC instability, with implications for other WBC systems under a warming climate.

Results

Synoptic evolution of Hurricanes Helene and Milton and Loop Current state

Hurricanes Helene and Milton followed distinct but overlapping trajectories through the GoM. Helene formed in the western Caribbean, entered the eastern Gulf, and then recurved toward the Florida coast between 24 and 27 September 2024, reaching Category 4 intensity with maximum sustained winds of ~120 kt[37] (see also Fig. 1a-c). Approximately eight days later, Milton formed in the central GoM on 5 October, rapidly intensified to Category 5 with winds exceeding 150 kt, and then weakened to Category 3 as it crossed the West Florida shelf and made landfall on 10 October[37] .

Before Helene entered the Gulf and LCE formed, the LC extended northward deep into the Gulf with a cyclonic Tortugas eddy near the Dry Tortugas region (Fig. 1a). The sea-surface height (SSH) field revealed a robust anticyclonic ridge associated with the LC–Eddy complex and a closed cyclonic trough marking the CE. Surface currents flowed strongly along the LC axis, while weaker cyclonic circulation characterized the CE. This pre-storm state set the stage for strong TC–mesoscale interactions.

As Helene and Milton traversed the basin, strong surface winds and low pressure generated large storm surges along the eastern Gulf coast and strong alongshore currents (Fig. S1; Fig. 1b,c). Elevated SSH followed the storm centers during the events due to the inverted barometer effect and wind-driven coastal setup (Fig. 1d). Helene's passage passed on the northern side of the CE that is to the right of the passage where the inertial response of greatest and left behind a

pronounced cold wake in SST outside the LC, which continued to grow after passage (Fig. 1f). Milton then went directly over the CE that was much cooler during 7th-10th October. On 10 October, coincident with Milton's landfall, the LC began shedding LCE Edison, indicated by a clear separation between the LC core and the eddy's SSH maximum and surface circulation in the model (Fig. 1d,e; Supplementary Fig. S2).

As Helene and Milton traversed the basin, strong surface winds and low pressure generated large storm surges along the eastern Gulf coast and strong alongshore currents (Fig. S1; Fig. 1b,c). Elevated SSH followed the storm centers due to the inverted barometer effect and wind-driven coastal setup (Fig. 1d). Helene passed on the northern side of the CE—to the right of the storm track, where the inertial response is greatest —leaving behind a pronounced cold wake in SST outside the LC. This cold wake continued to grow after passage (Fig. 1f). Milton then passed directly over the CE, which was substantially cooler during 7–10 October. On 10 October, coincident with Milton's landfall, the LC began shedding LCE Edison. This was indicated by a clear separation between the LC core and the eddy's SSH maximum and surface circulation in the model (Fig. 1d,e; Supplementary Fig. S2).

Upper-ocean cooling and nonlinear storm interactions

We quantified the TCs' impact on upper-ocean thermodynamics by comparing SST fields from the control simulation with those from the no-hurricane, no-Helene, and no-Milton experiments (Table 1, Fig. 2). The difference between the control and no-hurricane runs represents the combined effect of Helene and Milton, while differences with the no-Helene and no-Milton runs isolate each storm's contribution.

Helene alone produced substantial SST reductions in the eastern GoM on 27 September and sustained to Hurricane Milton period, particularly along and to the right of its track and over the West Florida shelf (Fig. 2c,g–i). Cooling of up to ~2 degrees was simulated outside the LC, consistent with classical hurricane responses controlled by wind-driven mixing and upwelling[21–25]. Cooling was strongest where mixed layers were initially shallow and winds were strongest, with relatively limited cooling within the warm LC core due to the deep layer of warm water compared to the entire West Florida shelf (Fig. S3b-c).

During Milton's period (8–10 October), the control run exhibited the most extensive cooling across the basin, especially over the shelf and along Milton's path (Fig. 2d–f). An average of ~0.4 and 0.5 °C cooling is observed in the Loop Current and shelf, respectively. The peak cooling was up to over 0.6 °C in both areas. In contrast, the Helene-only experiment (no-Milton run) produced noticeably weaker cooling (even warming) in the eastern Gulf and over the West Florida shelf (<0.2 °C, Fig. 2j–l). The Milton-only experiment (no-Helene run) showed that Helene's cooling remained detectable throughout the Milton period, particularly over the shelf and near the LC boundary (Fig. 2g–i). These results indicate that Helene preconditioned the upper ocean for Milton by creating a large cold anomaly that reduced surface enthalpy fluxes and

likely contributed to Milton's weakening over the cooled CE and the shelf, consistent with previous examples of storms encountering cold wakes and eddies[25,30] .

Comparing the sum of the Helene-only and Milton-only responses with the full control-minus-no-hurricane signal (Supplementary Fig. S4) reveals clear nonlinearity: the combined effect of both storms is not equivalent to the simple linear superposition of their individual impacts. This arises because Helene modifies the stratification and mesoscale eddy field, which in turn alters Milton's mixing efficiency, Ekman pumping, and surface fluxes. Such sensitivity to pre-existing ocean conditions has been emphasized for storm intensity evolution[25,30,31]; our results show that it also shapes the ocean's mesoscale and LC-WBC response.

Cyclonic eddy intensification and vertical structure

Helene's passage induced strong cooling and vertical mixing near the Tortugas CE, enhancing its cyclonic vorticity (Fig. S5) and modifying its vertical structure (Fig. S7). Vertical temperature sections across the LC–CE system (Supplementary Fig. S7) show a shoaling of isotherms within the CE, shallowing of the mixed layer, and a sharpening of the cross-frontal density gradient between the CE and the adjacent LC under the Hurricanes' forcing. Such changes decrease available potential energy of CE (Fig. S6) and favor baroclinic instability along the LC's northern flank.

The intensification of the CE is consistent with theoretical expectations that storm-induced upwelling and Ekman pumping can inject cyclonic vorticity and strengthen cold-core structures[21,25,32]. In our simulations, the strengthened Tortugas CE persisted for more than a week after Helene, maintaining a cool, cyclonic anomaly that acted as a negative feedback on Milton's intensification by reducing SST and surface enthalpy fluxes along part of its track, similar to the role of cold eddies under storms such as Idalia[30].

Loop Current weakening and accelerated eddy shedding

Beyond thermodynamics, Helene and Milton substantially modified the LC's dynamical structure. Differences in SSH and surface currents between the control and no-hurricane runs (Fig. 3a–f) show that during the storms the GoM experienced elevated SSH along the storm paths and near the coast. After their passage, however, SSH over the LC region became depressed (e.g., Fig. 3c, f), and the LC–LCE system exhibited enhanced cyclonic anomalies (Fig. S5c, f) and weakened anticyclonic circulation, particularly along the LC's northern flank. Approximate 28% (87%) more positive vorticity was injected into the LC-LCE (Eastern GoM) system during the hurricane simulation period to intensify the CE and weaken the LC (Fig. S3).

In the LC region, negative SSH anomalies developed and intensified following Helene, and the anticyclonic circulation associated with the LC–LCE system slowed. The shoaling of isotherms within and around the Tortugas CE, and the enhanced lateral density gradients at the interface with the LC (Fig. S7), are indicative of increased baroclinic instability. These structural changes

facilitated the early detachment of LCE Edison on 10 October, as seen in the separation of closed SSH contours between the LC core and the eddy and the emergence of distinct surface circulation patterns (Fig. 1d,e; Fig. S2).

In the no-hurricane experiment, the LC still eventually shed Edison but at 6 days later and with weaker CE intensification (Figure. S2). This comparison suggests that the storms accelerated the LC's transition from a strongly attached LCE configuration to a detached eddy state. Conceptually, TC forcing nudges the LC system across a stability threshold by weakening the anticyclonic LC–LCE structure and strengthening competing cyclonic eddies.

Distinct roles of Helene and Milton

The hurricane-denial experiments (Table 1; Fig. 3g–l) allow us to separate Helene's and Milton's contributions. In terms of the Helene's impact alone, the LC continued to weaken for more than a week after Helene, even without Milton's forcing (Fig. 3g–i). The near-inertial currents was excited by Helene to its right side and persisted after Helene's landfall. Similar inertial response of cold wake has been observed by many previous studies for other TCs [26,29]. SSH anomalies over the LC–LCE system became increasingly negative, and anticyclonic flow slowed, while the Tortugas CE strengthened and expanded. This prolonged response reflects the relatively slow adjustment of the upper-ocean density structure following intense mixing and upwelling, similar to delayed mesoscale responses seen after sequential storms in other regions[25] .

With respect to the Milton's solo impact, Milton generated a broader SSH response across the GoM, but its pre-detachment influence on LC structure and CE strength that can be both seen in the horizontal pattern (Fig. 2-3) and vertical temperature structure (Fig. S7) was smaller than Helene's (Fig. 3j–l). Milton's solo impact caused the late strengthening of CE and thus late detachment of LCE Edison compared to Helene's solo impact (Fig. S2). Taken together, these results show that Helene played the primary role in weakening the LC and intensifying the Tortugas CE, thereby conditioning the system for earlier eddy shedding, whereas Milton acted mainly to amplify and re-organize mesoscale anomalies that Helene had already generated.

Discussion

Tropical cyclones as amplifiers of mesoscale variability

Our results provide quantitative evidence that TCs can substantially enhance mesoscale eddy activity within a WBC system by altering both thermodynamics and dynamics. Helene's passage produced strong SST cooling and vertical mixing, intensified an existing CE, and sharpened frontal density gradients—a combination that increased baroclinic instability and weakened the LC. Milton's subsequent passage reinforced these anomalies and coincided with the early detachment of LCE Edison. This behavior is consistent with previous demonstrations that storm-induced upwelling and Ekman pumping can inject cyclonic vorticity and modify mesoscale eddies[21,25,32], but here we extend this understanding to include the eddy-shedding dynamics of a major WBC.

The combined response to Helene and Milton is distinctly nonlinear. Simple superposition of Helene-only and Milton-only simulations fails to reproduce the full cooling and SSH anomalies (Fig. S4), underscoring that storm sequencing and ocean preconditioning matter. The intermediate state of the eddy field after Helene—stronger CE, weakened LC—creates a distinct ocean background that modifies how Milton's forcing projects onto mesoscale modes. Similar sensitivity of hurricane intensity to pre-existing ocean structure has been documented for storms such as Michael, Ian, and Hai-Tang[19,20,25,31]; our results show that this sensitivity also shapes the LC's mesoscale and stability response.

Climate-change implications for hurricane–eddy interactions

Multiple studies suggest that anthropogenic warming is likely to increase the frequency of rapid intensification events and the proportion of high-intensity TCs, even if changes in overall TC frequency are less certain[17,18,34–36]. In a warmer climate with increased upper-ocean heat content and more frequent intense storms, the type of hurricane–eddy interactions documented here may become more common. Enhanced TC-driven mixing and vorticity injection could lead to greater mesoscale variability, more frequent or earlier eddy shedding, and altered pathways of heat and salt transport by WBCs.

For the LC in particular, changes in LCE shedding statistics can influence regional sea-level variability, offshore platform risk, and downstream Gulf Stream dynamics. Our findings therefore suggest that TC–WBC coupling should be considered as a potential feedback in climate projections of regional ocean circulation and extremes, complementing existing work on TC motion, intensity, and track shifts[34–36].

Implications for predictability and hazard forecasting

TC-induced modifications of the LC and its eddies have implications for both atmospheric and oceanic predictability. From the atmospheric side, the upper-ocean structure along prospective storm tracks is a key control on intensity evolution[14,15,19–21,25]. Our results show that previous

storms can precondition this structure by cooling the surface and altering mesoscale eddies, thereby affecting subsequent storms—a multi-storm memory effect similar to that seen for sequential typhoons[25].

From the oceanic side, LC state transitions are notoriously difficult to predict, yet they strongly affect offshore operations, surface drift, and risk assessments. By showing that strong TCs can accelerate eddy shedding, this study highlights the need to represent storm–eddy coupling in operational ocean forecast systems such as CNAPS2[38]. Improved assimilation of altimetry, SST, and subsurface profile data, as well as new datasets such as SWOT into high-resolution coupled models[30] could enhance our ability to anticipate both TC intensity changes and major LCE shedding events.

Conceptual framework: hurricanes as modulators of western boundary current instability

Figure 4 summarizes the sequence of processes inferred from the simulations and feature-denial experiments performed in this study. Before the storms, the LC supports a large warm eddy and a weaker Tortugas CE. Helene's strong winds and surface forcing cool the upper ocean outside the LC, deepen and intensify the CE, and weaken the LC–LCE system. The enhanced density gradient and cyclonic shear along the LC's northern flank increase baroclinic instability and favor eddy detachment. Milton then interacts with this preconditioned state, further cooling and redistributing the mesoscale field but playing a secondary role in initiating LCE (Edison) separation. The net effect is an amplification of mesoscale variability and an acceleration of LC instability due to sequential TC forcing.

Limitations and future directions

While our model configuration captures the observed timing of LCE Edison detachment and reproduces the broad patterns of SST and SSH anomalies, uncertainty remains regarding vertical mixing parameterizations, air–sea flux formulations, and the representation of submesoscale processes. Subsurface profile data in the CEs during hurricane passage could validate some of the model simulations. We have focused on a single, albeit striking, pair of storms. Extending this analysis to a larger ensemble of TC–LC interactions, and to other WBC systems such as the Kuroshio or Agulhas, will be crucial to assess the generality of our conclusions. Coupled atmosphere–ocean simulations and targeted observations during and after storms will be essential to close the loop between atmospheric forcing, ocean response, and subsequent storm evolution.

Methods

Regional ocean model configuration

We use a high-resolution implementation of the Regional Ocean Modeling System (ROMS) configured as part of the Coupled Northwest Atlantic Prediction System 2.0 (CNAPS2)[38]. The model domain covers the GoM and adjacent portions of the northwest Atlantic, with a horizontal grid spacing of 1/25° (~4 km), sufficient to resolve mesoscale eddies and major LC meanders. The model employs terrain-following sigma coordinates, which provide enhanced resolution in the upper ocean and near the bottom boundary to better capture mixed-layer processes and topographic effects.

ROMS solves the hydrostatic, Boussinesq primitive equations with a split-explicit free-surface scheme, third-order upstream-biased advection, and a turbulence closure scheme for vertical mixing. The time step is chosen to satisfy stability constraints for both barotropic and baroclinic modes. Vertical grid spacing is refined near the surface and bottom to better represent mixed-layer dynamics and bottom boundary layer processes.

The simulation period spans 23 September–23 October 2024, covering the formation, intensification, and landfall of Hurricanes Helene and Milton, as well as the detachment of LCE Edison. The initial ocean state and open boundary conditions are taken from the Copernicus GLORYS12V1 global ocean reanalysis, which provides 3D temperature, salinity, and velocity fields with realistic LC and mesoscale eddy structure at the start of the integration. Open boundaries are treated using a combination of radiation and nudging conditions to maintain consistency with large-scale circulation while allowing mesoscale variability to evolve freely within the domain.

Atmospheric forcing is derived from the European Centre for Medium-Range Weather Forecasts (ECMWF) ERA5 reanalysis, which provides hourly global fields of 10-m winds, sea-level pressure, surface air temperature and humidity, and radiative fluxes. Bulk formulae are applied to compute turbulent heat and momentum fluxes at the ocean surface. This forcing captures the evolving wind and pressure fields associated with both Helene and Milton, as well as background synoptic variability. Storm tracks and intensities (Fig. S1) are consistent with the International Best Track Archive for Climate Stewardship (IBTrACS) and National Hurricane Center reports[37] .

To ensure that the modeled LC system and storm responses are realistic, we qualitatively compare SSH and surface current fields with available satellite altimetry and surface products during the LCE detachment period (Fig. S1). The modeled LC path, LCE Edison detachment date, and large-scale SSH patterns agree with operational assessments of LC eddies, lending confidence to the simulations. Modeled SST cooling magnitudes and spatial patterns are also consistent with observed hurricane wake behavior in the GoM and other basins[21–25,30].

Hurricane-denial sensitivity experiments

To isolate the individual contributions of Helene and Milton, we performed a suite of experiments summarized in Table 1:

- **Control run:** Full ERA5 forcing is applied throughout the simulation, including realistic wind and pressure fields associated with both hurricanes (see also Fig. S1a,c).
- **No-Helene run:** ERA5 fields are used except during Helene's active period (26–27 September), when wind and pressure anomalies associated with the storm are replaced with climatological values representative of typical conditions for that time of year (Fig. S1b).
- **No-Milton run:** ERA5 fields are used except during Milton's active period (8–10 October), when its wind and pressure anomalies are similarly replaced by climatology (Fig. S1d).
- **No-hurricane run:** Both Helene and Milton periods are forced with climatological fields, while the rest of the simulation retains realistic ERA5 forcing.

In practice, we identify storm periods based on best-track data and then remove the corresponding ERA5 anomalies. Differences between the control and each sensitivity run quantify the direct impact of each storm on SST, SSH, surface currents, and vertical structure.

$$X_{Helene\ impact} = X_{Control} - X_{No\ Helene} \quad (1)$$

$$X_{Milton\ impact} = X_{Control} - X_{No\ Milton} \quad (2)$$

$$X_{Hurricane\ impact} = X_{Control} - X_{No\ Hurricane} \quad (3)$$

where X can be any model output or derived variables.

The difference between the control and no-hurricane runs yields the combined effect of both storms, while comparison with the sum of the Helene-only and Milton-only impacts (Fig. S4) reveals nonlinear interactions.

Eddy identification

We diagnosed cyclonic and anticyclonic eddies using closed SSH contours (0.4 m) relative to a background level, complemented by relative vorticity fields (ζ) calculated as:

$$\zeta = \frac{\partial v}{\partial x} - \frac{\partial u}{\partial y} \quad (4)$$

where u and v represent the eastward and northward velocity components (m s^{-1}), respectively, and x and y denote the eastward and northward distances (m). Positive values of ζ indicate

cyclonic rotation (counterclockwise in the Northern Hemisphere), while negative values indicate anticyclonic rotation. The relative vorticity is then normalized by Coriolis number f for further comparison.

LCE Edison is identified as a large, closed anticyclonic SSH maximum; the Tortugas CE is defined as a persistent closed cyclonic minimum near the Dry Tortugas region.

Ocean Heat Content

Ocean heat content (OHC) was calculated to quantify the thermal energy stored in the water column. The OHC represents the integrated heat anomaly relative to a reference temperature and was computed as:

$$OHC = \int_0^H \rho\, C_{\mathrm{p}}(T - T_{ref})\,dz \quad (5)$$

where ρ is the seawater density (kg m^{-3}), C_{p} is the specific heat capacity of seawater at constant pressure (J kg^{-1} K^{-1}), T is the in-situ temperature at depth z (°C), T_{ref} is the reference temperature (12°C), H is the maximum integration depth (m), and z is the vertical coordinate (m). For this study, we used ρ = 1025 kg m^{-3} and C_{p} = 3990 J kg^{-1} K^{-1}, which are representative values for seawater. Integration was performed from the surface (z = 0) to the depth of T_{ref} (12°C isotherm). The resulting OHC is expressed in units of kJ cm^{-2}.

Data availability

Model output from the control and sensitivity experiments will be made publicly available at [repository/link would be provided upon acceptance]. ERA5 atmospheric reanalysis can be obtained from the ECMWF Climate Data Store (https://cds.climate.copernicus.eu/datasets/reanalysis-era5-single-levels). GLORYS12V1 ocean reanalysis fields are available from the Copernicus Marine Service (https://data.marine.copernicus.eu/product/GLOBAL_MULTIYEAR_PHY_001_030). Best-track hurricane data are available from the National Hurricane Center and IBTrACS archives (https://www.ncei.noaa.gov/products/international-best-track-archive).

Code availability

The ROMS configuration files and analysis scripts used in this study are available from the corresponding author upon reasonable request and will be deposited in a public repository upon publication.

References (Nature / Nat. Commun. numbered style)

1. Wu, L. *et al*. Enhanced warming over the global subtropical western boundary currents. *Nature Clim Change* **2**, 161–166 (2012).

2. Hu, D. *et al*. Pacific western boundary currents and their roles in climate. *Nature* **522**, 299–308 (2015).

3. Parfitt, R. & Seo, H. A New Framework for Near-Surface Wind Convergence Over the Kuroshio Extension and Gulf Stream in Wintertime: The Role of Atmospheric Fronts. *Geophysical Research Letters* **45**, 9909–9918 (2018).

4. Wills, S. M., Thompson, D. W. J. & Ciasto, L. M. On the Observed Relationships between Variability in Gulf Stream Sea Surface Temperatures and the Atmospheric Circulation over the North Atlantic. *Journal of Climate* **29**, 3719–3730 (2016).

5. Talley, L. D. Shallow, Intermediate, and Deep Overturning Components of the Global Heat Budget. https://journals.ametsoc.org/view/journals/phoc/33/3/1520-0485_2003_033_0530_siadoc_2.0.co_2.xml (2003).

6. Oey, L.-Y. *et al*. An exercise in forecasting loop current and eddy frontal positions in the Gulf of Mexico. *Geophysical Research Letters* **32**, (2005).

7. Elliott, B. A. Anticyclonic Rings in the Gulf of Mexico. https://journals.ametsoc.org/view/journals/phoc/12/11/1520-0485_1982_012_1292_aritgo_2_0_co_2.xml (1982).

8. Forristall, G. Z., Schaudt, K. J. & Cooper, C. K. Evolution and kinematics of a loop current eddy in the Gulf of Mexico during 1985. *Journal of Geophysical Research: Oceans* **97**, 2173–2184 (1992).

9. Vukovich, F. M. & Maul, G. A. Cyclonic Eddies in the Eastern Gulf of Mexico. https://journals.ametsoc.org/view/journals/phoc/15/1/1520-0485_1985_015_0105_ceiteg_2_0_co_2.xml (1985).

10. Fratantoni, P. S., Lee, T. N., Podesta, G. P. & Muller-Karger, F. The influence of Loop Current perturbations on the formation and evolution of Tortugas eddies in the southern Straits of Florida. *Journal of Geophysical Research: Oceans* **103**, 24759–24779 (1998).

11. Jouanno, J. *et al*. Loop Current Frontal Eddies: Formation along the Campeche Bank and Impact of Coastally Trapped Waves. https://doi.org/10.1175/JPO-D-16-0052.1 (2016) doi:10.1175/JPO-D-16-0052.1.

12. Le Hénaff, M., Kourafalou, V. H., Morel, Y. & Srinivasan, A. Simulating the dynamics and intensification of cyclonic Loop Current Frontal Eddies in the Gulf of Mexico. *Journal of Geophysical Research: Oceans* **117**, (2012).

13. Emanuel, K. Tropical cyclone energetics and structure. in *Atmospheric Turbulence and Mesoscale Meteorology: Scientific Research Inspired by Doug Lilly* (eds Stevens, B., Fedorovich, E. & Rotunno, R.) 165–192 (Cambridge University Press, Cambridge, 2004). doi:10.1017/CBO9780511735035.010.

14. Anthes, R. A. & Chang, S. W. Response of the Hurricane Boundary Layer to Changes of Sea Surface Temperature in a Numerical Model. https://journals.ametsoc.org/view/journals/atsc/35/7/1520-0469_1978_035_1240_rothbl_2_0_co_2.xml (1978).

15. Emanuel, K. A. Thermodynamic control of hurricane intensity. *Nature* **401**, 665–669 (1999).

16. Glenn, S. M. *et al*. Stratified coastal ocean interactions with tropical cyclones. *Nat Commun* **7**, 10887 (2016).

17. Bhatia, K. *et al*. A potential explanation for the global increase in tropical cyclone rapid intensification. *Nat Commun* **13**, 6626 (2022).

18. Bhatia, K. T. *et al*. Recent increases in tropical cyclone intensification rates. *Nat Commun* **10**, 635 (2019).

19. Le Hénaff, M. *et al*. The Role of the Gulf of Mexico Ocean Conditions in the Intensification of Hurricane Michael (2018). *JGR Oceans* **126**, e2020JC016969 (2021).

20. Liu, Y., Weisberg, R. H., Sorinas, L., Law, J. A. & Nickerson, A. K. Rapid Intensification of Hurricane Ian in Relation to Anomalously Warm Subsurface Water on the Wide Continental Shelf. *Geophysical Research Letters* **52**, e2024GL113192 (2024).

21. Price, J. F. Upper Ocean Response to a Hurricane. https://journals.ametsoc.org/view/journals/phoc/11/2/1520-0485_1981_011_0153_uortah_2_0_co_2.xml (1981).

22. Shay, L. K., Black, P. G., Mariano, A. J., Hawkins, J. D. & Elsberry, R. L. Upper ocean response to Hurricane Gilbert. *J. Geophys. Res.* **97**, 20227–20248 (1992).

23. Hu, C. & Muller-Karger, F. E. Response of sea surface properties to Hurricane Dennis in the eastern Gulf of Mexico. *Geophysical Research Letters* **34**, (2007).

24. Zhang, H. *et al*. Upper ocean response to typhoon Kalmaegi (2014). *JGR Oceans* **121**, 6520–6535 (2016).

25. Wu, R. & Li, C. Upper ocean response to the passage of two sequential typhoons. *Deep Sea Research Part I: Oceanographic Research Papers* **132**, 68–79 (2018).

26. Yang, Y. J. *et al*. The role of enhanced velocity shears in rapid ocean cooling during Super Typhoon Nepartak 2016. *Nat Commun* **10**, 1627 (2019).

27. Shay, L. K., Mariano, A. J., Jacob, S. D. & Ryan, E. H. Mean and Near-Inertial Ocean Current Response to Hurricane Gilbert. https://journals.ametsoc.org/view/journals/phoc/28/5/1520-0485_1998_028_0858_manioc_2.0.co_2.xml (1998).

28. Shay, L. K. & Elsberry, R. L. Near-Inertial Ocean Current Response to Hurricane Frederic. https://journals.ametsoc.org/view/journals/phoc/17/8/1520-0485_1987_017_1249_niocrt_2_0_co_2.xml (1987).

29. Hormann, V., Centurioni, L. R., Rainville, L., Lee, C. M. & Braasch, L. J. Response of upper ocean currents to Typhoon Fanapi. *Geophysical Research Letters* **41**, 3995–4003 (2014).

30. Gopalakrishnan, G., Trott, C. B., Cruz, E. & Subrahmanyam, B. Understanding Ocean Surface Response to Hurricane Idalia Using SWOT Altimetry in the Gulf of Mexico. *Geophysical Research Letters* **52**, e2024GL114423 (2025).

31. Zheng, Z., Ho, C. & Kuo, N. Importance of pre-existing oceanic conditions to upper ocean response induced by Super Typhoon Hai-Tang. *Geophysical Research Letters* **35**, (2008).

32. Jaimes, B. & Shay, L. K. Enhanced Wind-Driven Downwelling Flow in Warm Oceanic Eddy Features during the Intensification of Tropical Cyclone Isaac (2012): Observations and Theory. *Journal of Physical Oceanography* **45**, 1667–1689 (2015).

33. Ni, X., Zhang, Y. & Wang, W. Hurricane influence on the oceanic eddies in the Gulf Stream region. *Nat Commun* **16**, 583 (2025).

34. Zhang, G., Murakami, H., Knutson, T. R., Mizuta, R. & Yoshida, K. Tropical cyclone motion in a changing climate. *Sci. Adv.* **6**, eaaz7610 (2020).

35. Knutson, T. *et al*. Tropical Cyclones and Climate Change Assessment: Part II: Projected Response to Anthropogenic Warming. *Bulletin of the American Meteorological Society* **101**, E303–E322 (2020).

36. Knutson, T. R. *et al.* Global Projections of Intense Tropical Cyclone Activity for the Late Twenty-First Century from Dynamical Downscaling of CMIP5/RCP4.5 Scenarios. *Journal of Climate* **28**, 7203–7224 (2015).

37. Andrew B. Hagen, John P. Cangialosi, Marc Chenard, Laura Alaka, & Sandy Delgado. *NATIONAL HURRICANE CENTER TROPICAL CYCLONE REPORT-HURRICANE HELENE*. https://www.nhc.noaa.gov/data/tcr/AL092024_Helene.pdf (2025).

38. He, R. *et al.* Advanced Ocean Reanalysis of the Northwestern Atlantic: 1993-2022. Preprint at https://doi.org/10.48550/arXiv.2503.06907 (2025).

Acknowledgements

This research was supported by the National Science Foundation (NSF) under grants RISE-2019758, OCE-2206052, OCE-2421624, CNS-2223844, and OAC-2417850. Additional support from the National Academies of Sciences, Engineering, and Medicine (NASEM) Gulf Research Program is gratefully acknowledged.

Author contributions

Y.D. and T.W. designed the experiments, carried out the simulations, and performed the analysis. Y.D. and T.W. equally contributed to this study. S.G. contributed to interpretation and revised the manuscript. R.H. conceived the study, supervised the research, and contributed to interpretation. Y.D. wrote the original manuscript. All authors discussed the results and jointly wrote and revised the manuscript.

Competing interests

The authors declare no competing interests.

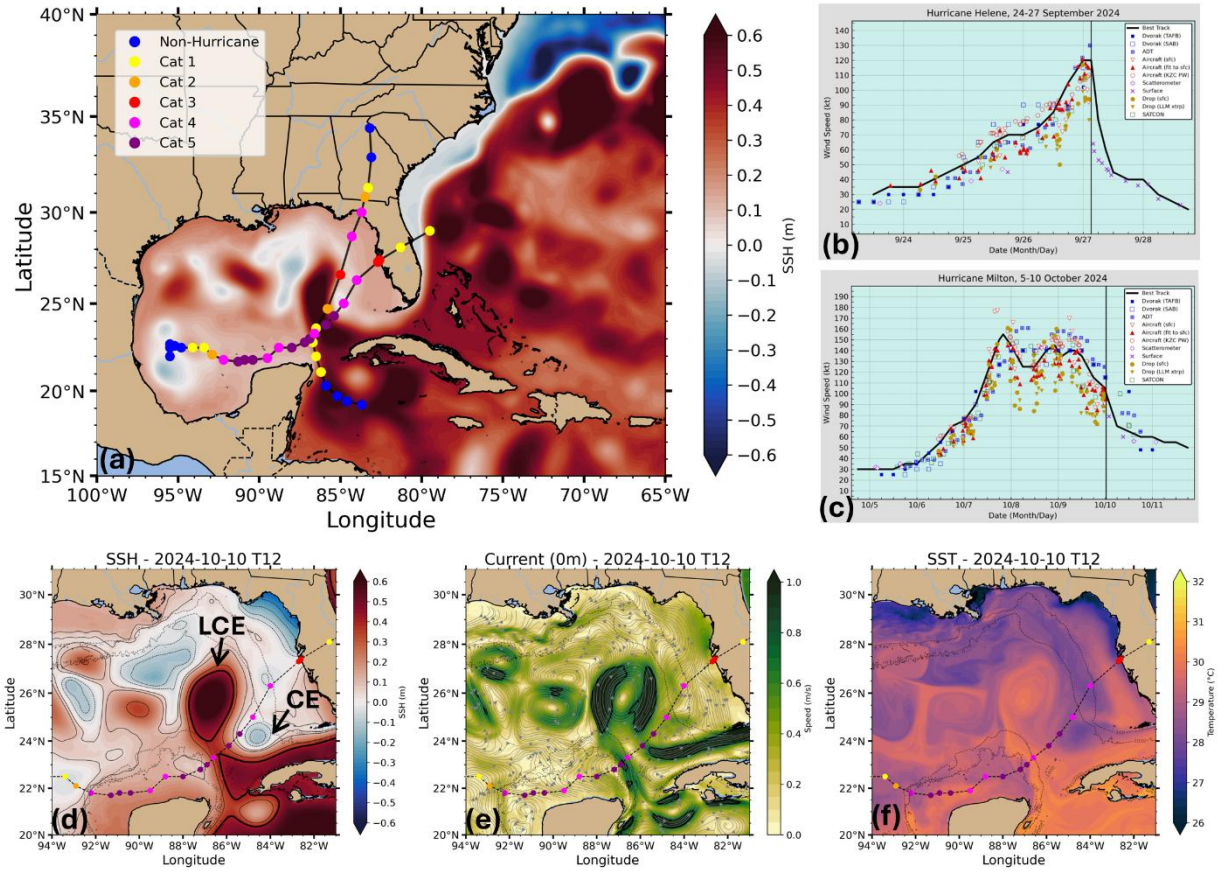

Figure 1 | Hurricanes Helene and Milton and Loop Current configuration.

a, Tracks of Hurricanes Helene and Milton overlaid on sea surface height (SSH) before Helene entered the Gulf of Mexico, showing the Loop Current (LC), Loop Current Eddy (LCE) Edison and the Tortugas cyclonic eddy. Hurricane tracks are from the International Best Track Archive for Climate Stewardship (IBTrACS), with symbols indicating Saffir–Simpson category. b,c, Time series of maximum sustained wind speed for Helene and Milton, respectively, from National Hurricane Center best-track data. d–f, SSH, surface currents and sea surface temperature (SST) on 10 October 2024, when LCE Edison detached from the LC. The maps highlight the separated warm eddy, the LC pathway and storm-induced cooling outside the LC.

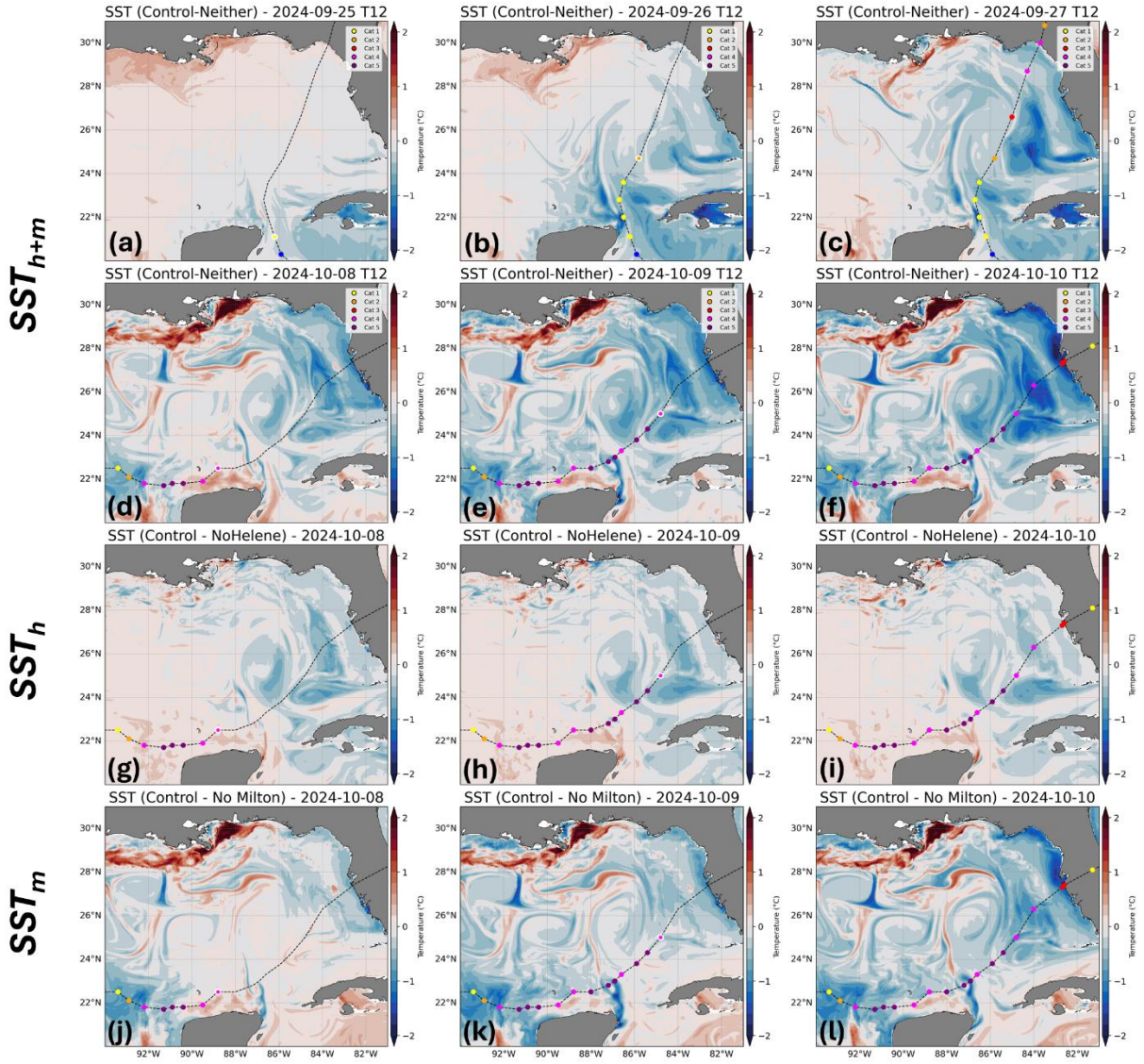

Figure 2 | Sea-surface temperature response to sequential hurricanes Helene and Milton.

SST differences between the control simulation and sensitivity experiments on selected dates. a–f, Control minus no-hurricane run, showing the combined effect of both storms. g–i, Control minus no-Helene run, isolating the contribution of Helene. j–l, Control minus no-Milton run, isolating the contribution of Milton. Blue (red) shading indicates cooling (warming) in the control simulation relative to each sensitivity experiment. The panels illustrate that Helene generates strong cooling in the eastern Gulf of Mexico and on the West Florida shelf, that this signal persists into the Milton period, and that the combined effect of both storms is nonlinear and larger than either alone.

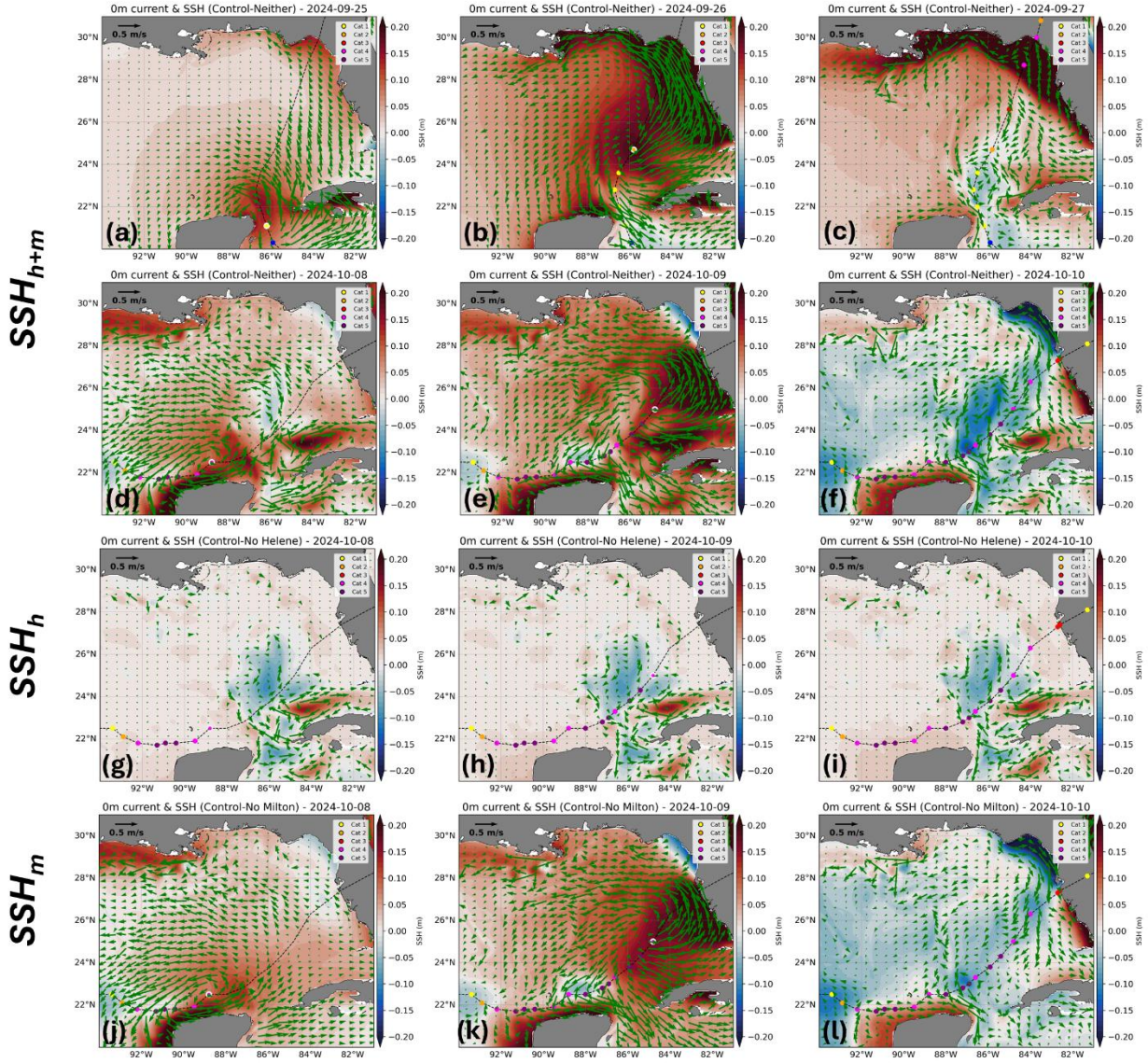

Figure 3 | Sea surface height and surface current anomalies driven by Helene and Milton.

Same as Figure 2 but for SSH and surface velocity. Negative SSH anomalies and enhanced cyclonic circulation along the LC's northern flank indicate LC weakening and Tortugas eddy intensification, with Helene exerting the dominant pre-detachment impact on LC structure.

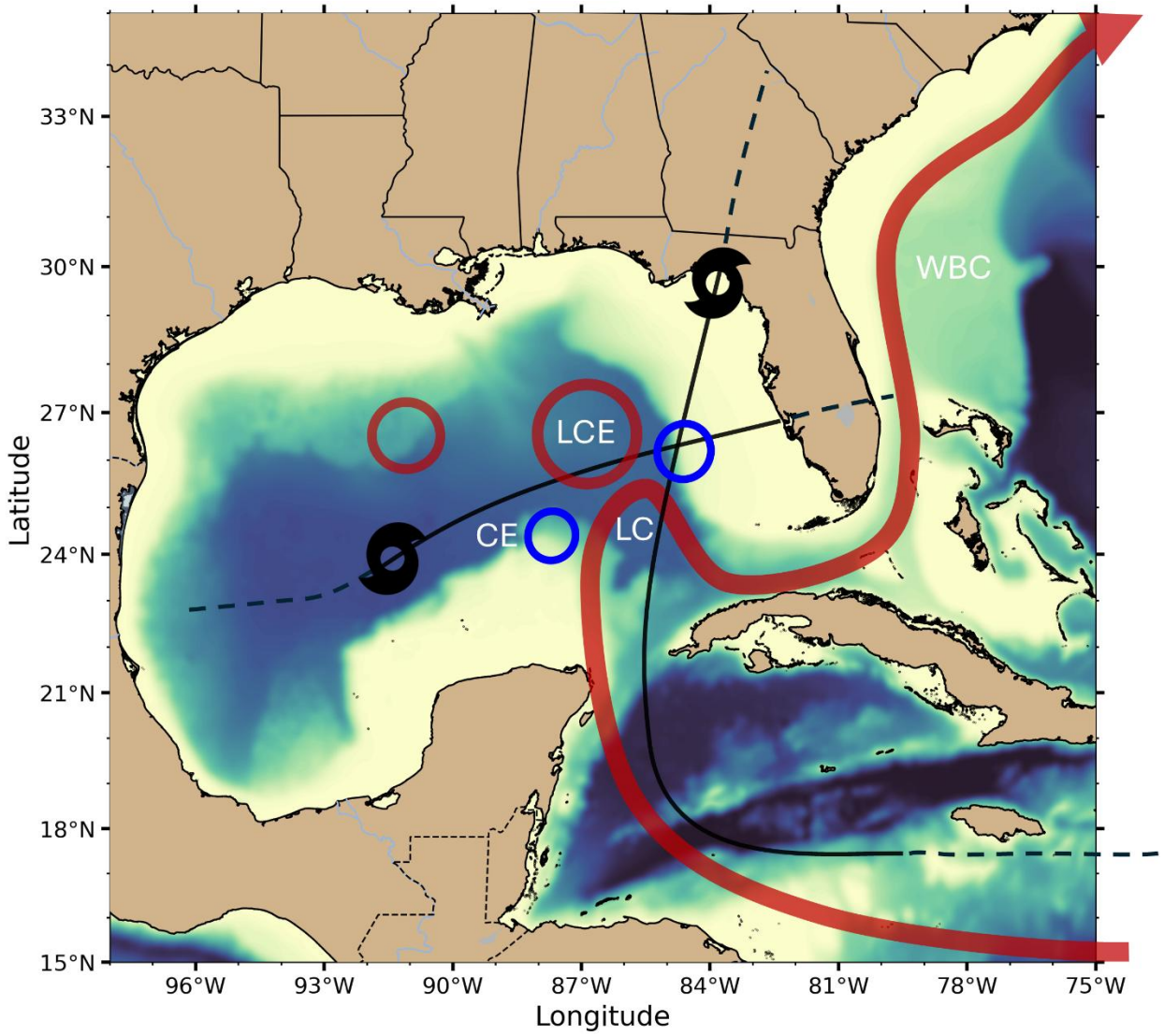

Figure 4 | Conceptual view of hurricane-driven mesoscale variability in the Loop Current system.

Schematic illustrating the evolution of the Loop Current (LC), Loop Current Eddy (LCE) Edison and the Tortugas cyclonic eddy in response to sequential hurricanes. Before the storms, the LC supports a large warm-core LCE and a weaker Tortugas eddy. Helene's passage cools the upper ocean outside the LC, deepens and strengthens the Tortugas eddy and weakens the LC–LCE system, sharpening frontal gradients and enhancing baroclinic instability. Milton then interacts with this preconditioned state, further cooling and reorganising the mesoscale field and coinciding with early detachment of LCE Edison. Red (blue) rings denotes warm (cold) eddies; arrows indicate LC and eddy circulation; black curves show schematic hurricane tracks.

Experiments	Helene period	Milton period	Other period	Comments
Control run	Real	Real	Real	All realistic forcing
No Helene	Clim.	Real	Real	Helene period forced by clim.
No Milton	Real	Clim.	Real	Milton period forced by clim.
No hurricane	Clim.	Clim.	Real	Both periods forced by clim.

Table 1 | Design of sensitivity experiments for Helene and Milton.

Summary of numerical experiments used to isolate the oceanic impacts of Hurricanes Helene and Milton. For each experiment, the type of atmospheric forcing applied during the Helene period (26–27 September 2024), the Milton period (8–10 October 2024) and all other times is indicated. "Real" denotes full ERA5 forcing including the storm-related wind and pressure anomalies, whereas "Clim." denotes climatological forcing representative of typical conditions for that time of year. The control run uses realistic forcing throughout, while the no-Helene, no-Milton and no-hurricane runs progressively remove the storms' signals to quantify their individual and combined effects.

Supporting Information for "Tropical cyclones intensify mesoscale eddy variability and accelerate Western Boundary Current instability"

Yongfei Deng[1], Tianning Wu[1], Scott Glenn[2], Ruoying He[1,*]

[1]Department of Marine, Earth, and Atmospheric Sciences, North Carolina State University, Raleigh, North Carolina, U.S. A.

[2]Department of Marine and Coastal Sciences, Rutgers University, New Brunswick, New Jersey, USA

Corresponding author: *rhe@ncsu.edu

Figure S1~S7

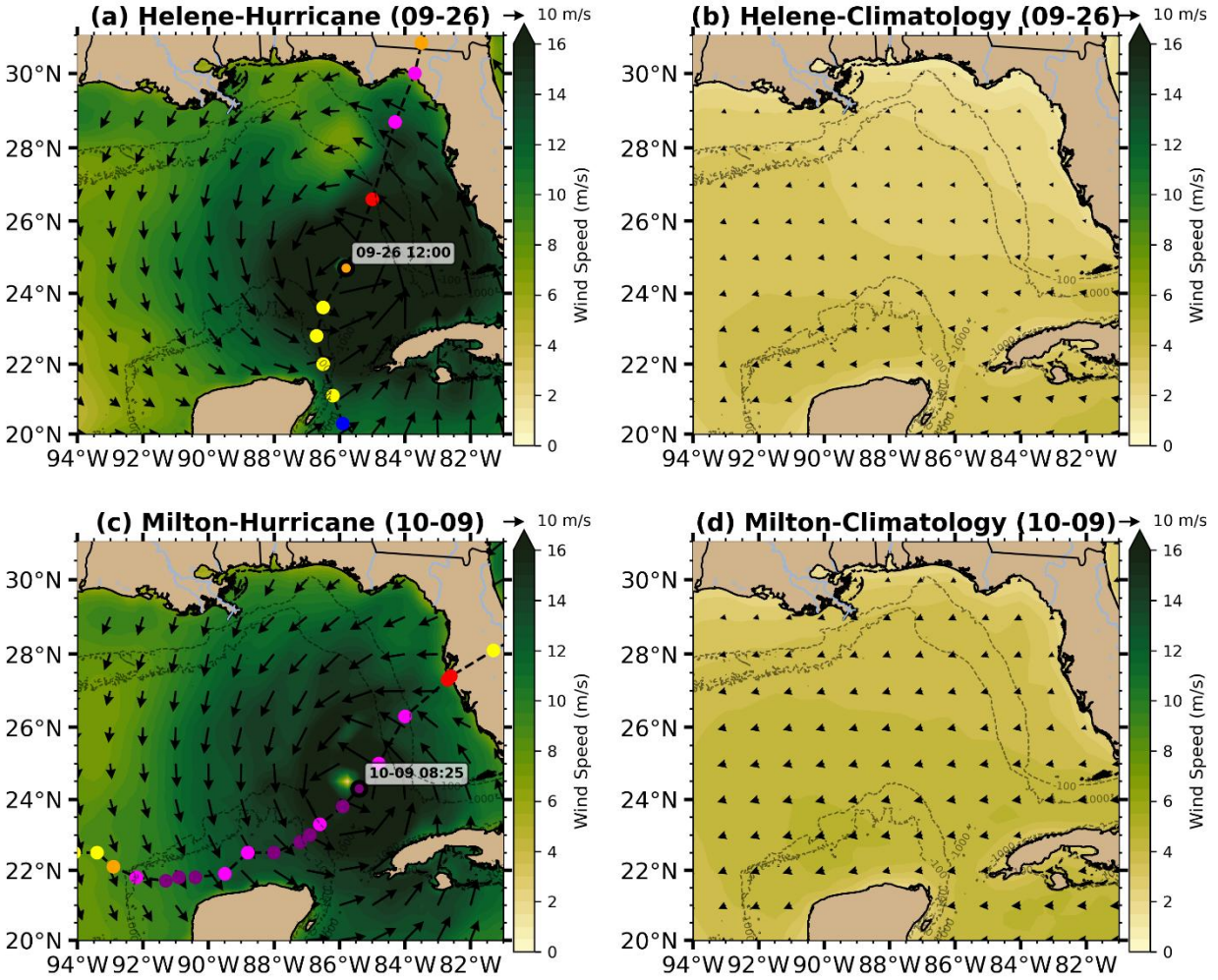

Figure S1. Surface winds over GoM during (a-b) Helene and (c-d) Milton periods. (a) and (c) are real wind forcing used for control run while (b) and (d) are climatological wind used for hurricane-denial experiments.

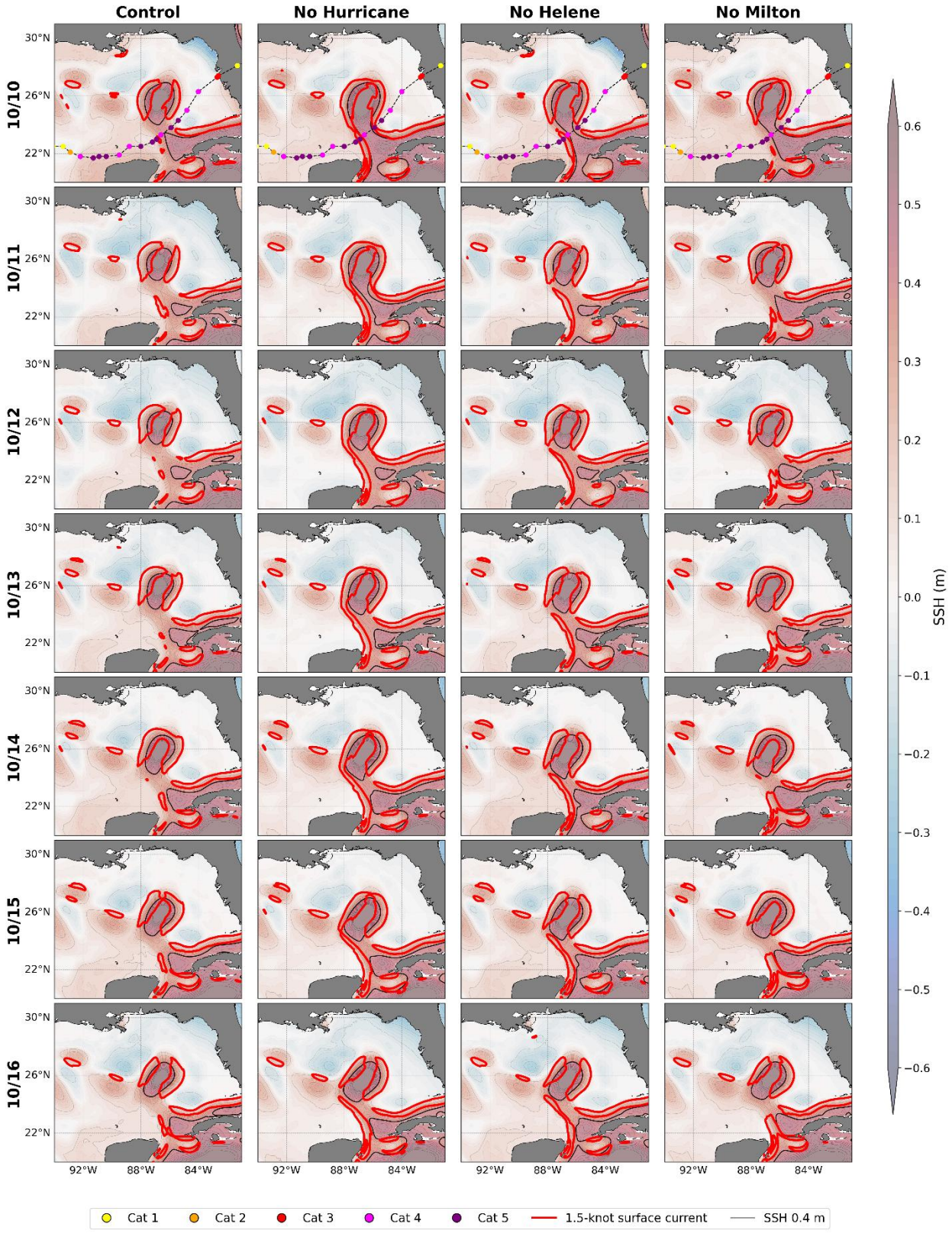

Figure S2. SSH and surface current during the Hurricane Milton period from Oct 10th through 16th 2024 for (first column) Control run; (second column) No-Hurricane run; (third column) No-

Helene run; (fourth column) No-Milton run. Hurricanes tracks, 0.4m SSH contour (black) and 1.5 knot current contour (red) are overlaid on the maps. Based on both criteria (SSH and current contour), the control run is determined to shed LCE Edison on 10/10; No-Hurricane run on 10/16; No-Helene run on 10/11; No-Milton run on 10/11.

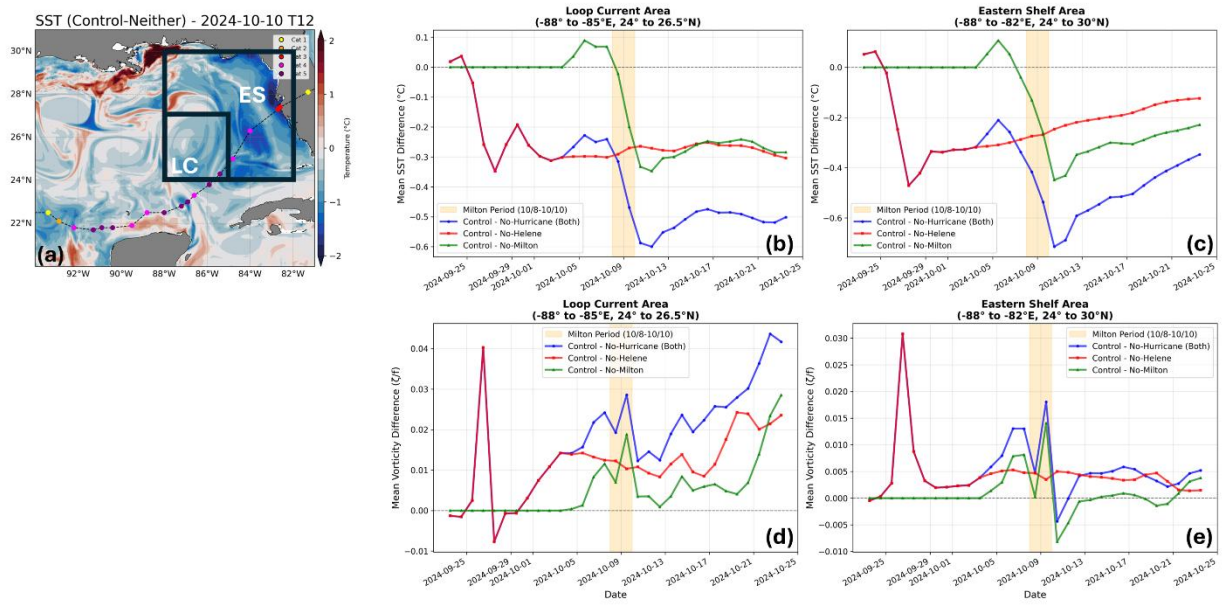

47

48 Figure S3. (a) A snapshot of SST difference (Control-No Hurricane) map showing the Loop
49 Current (LC) area and East Shelf (ES) area selected for computation of area-averaged time
50 series. (b-c) Time series of mean SST difference for LC and ES. (d-e) Time series of mean
51 vorticity (ζ/f) difference for LC and ES. The orange shading area highlights the Milton period.

52

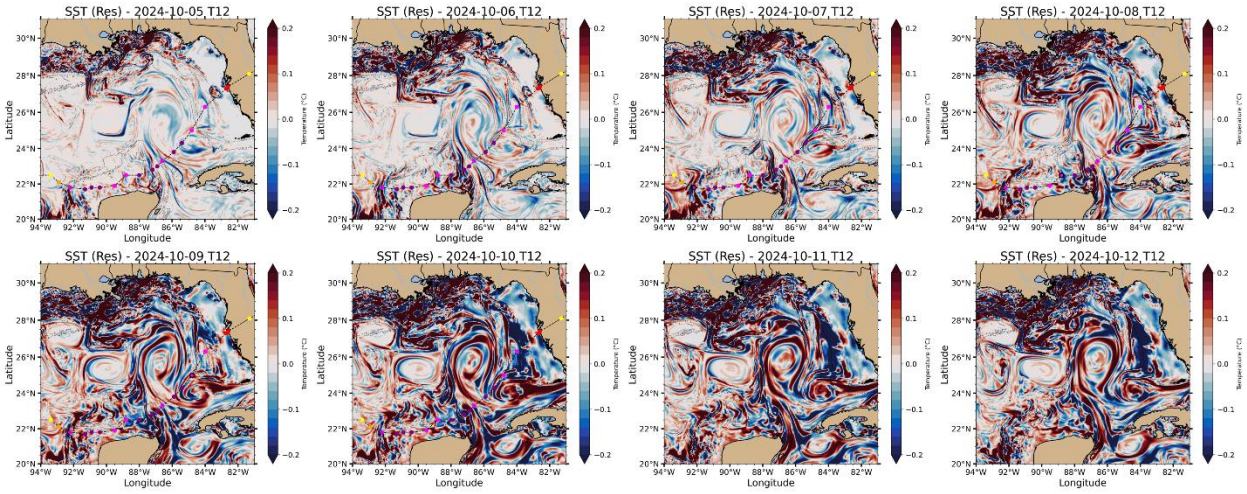

53

54 Figure S4. The SST difference between the sum of No-Helene and No-Milton run, and No-
55 hurricane run over the period Oct 5th through 12th 2024.

56

57

58

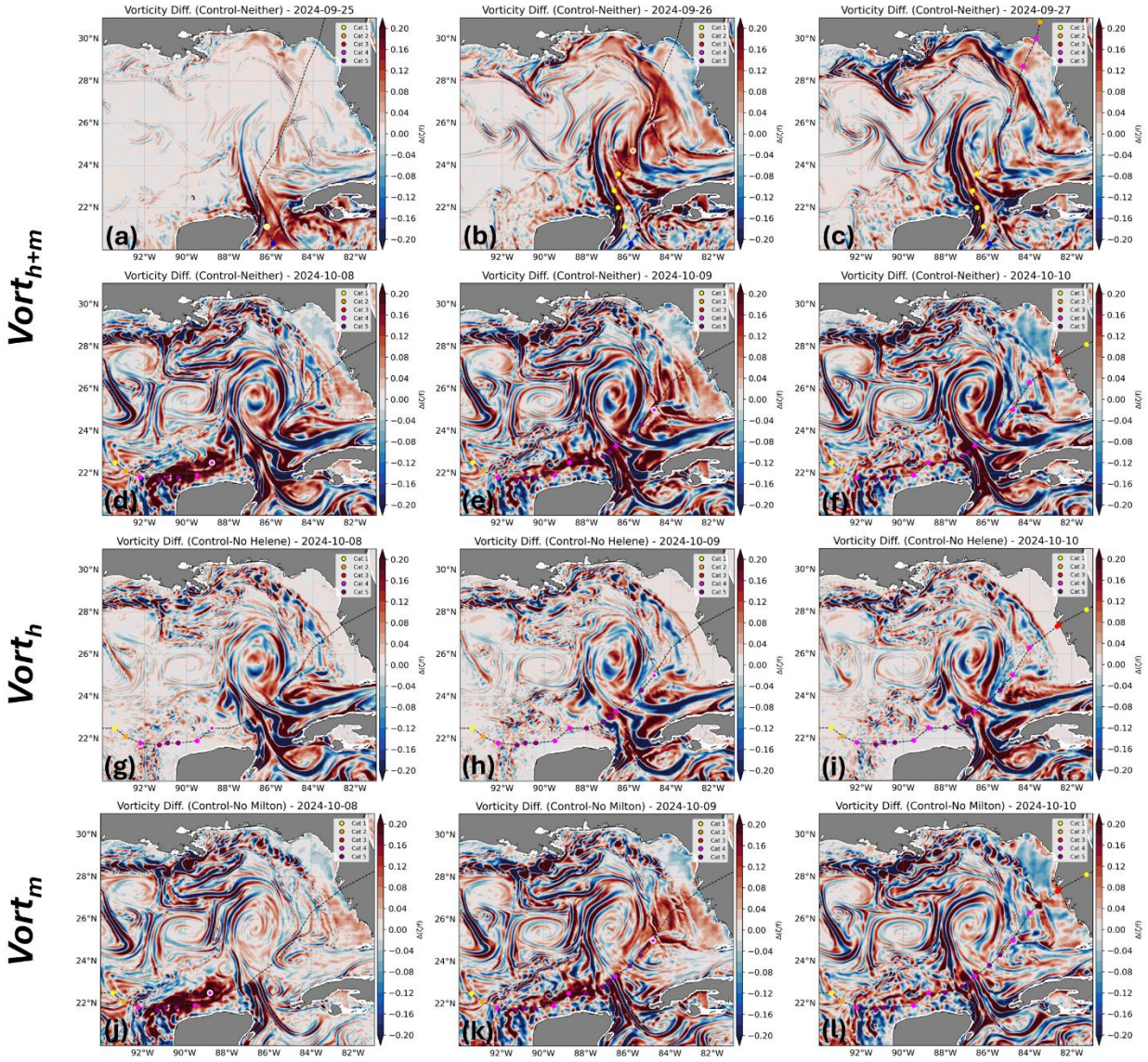

Figure S5. Vorticity response to sequential hurricanes Helene and Milton. Vorticity differences between the control simulation and sensitivity experiments on selected dates. a–f, Control minus no-hurricane run, showing the combined effect of both storms. g–i, Control minus no-Helene run, isolating the contribution of Helene. j–l, Control minus no-Milton run, isolating the contribution of Milton.

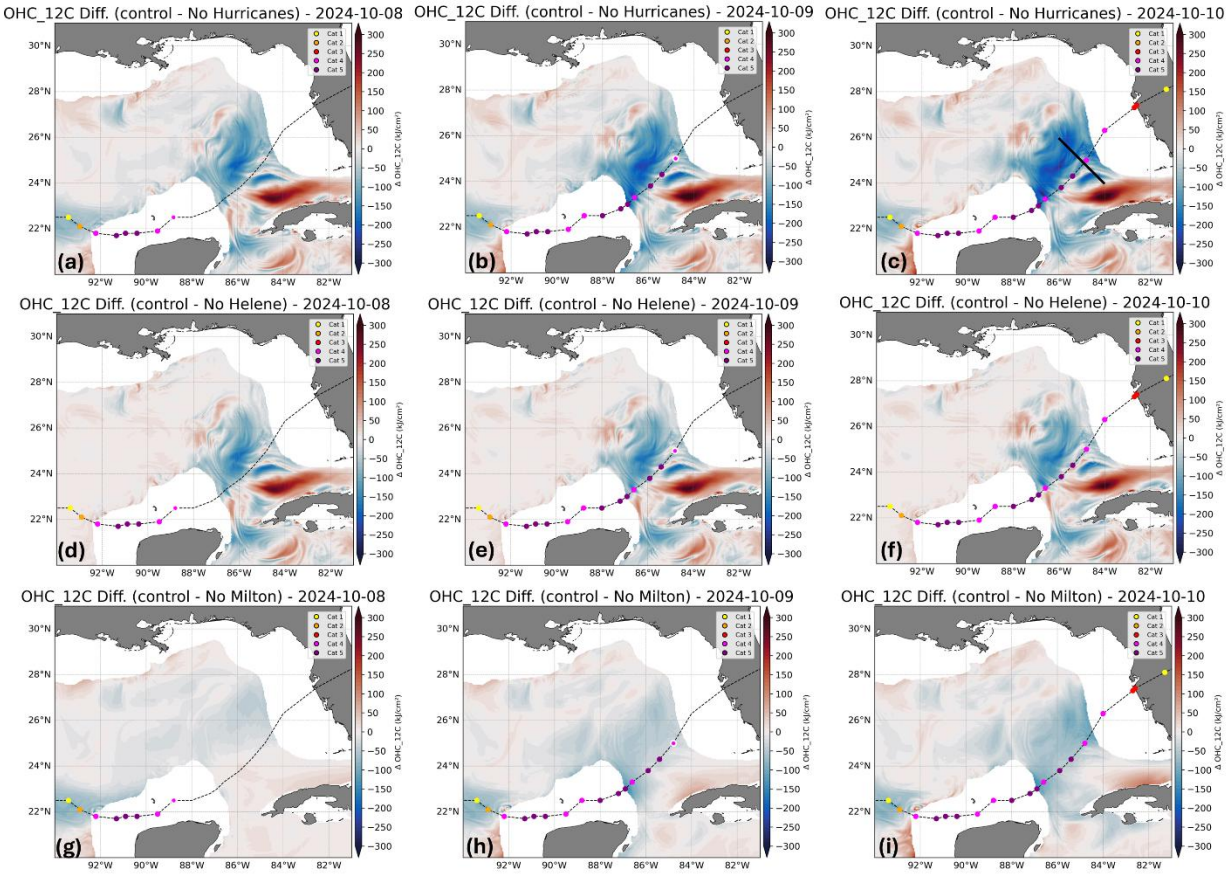

Figure S6. Ocean Heat Content (OHC) response to sequential hurricanes Helene and Milton over the period Oct 8th-10th 2024. OHC differences between the control simulation and sensitivity experiments on selected dates. a–f, Control minus no-hurricane run, showing the combined effect of both storms. g–i, Control minus no-Helene run, isolating the contribution of Helene. j–l, Control minus no-Milton run, isolating the contribution of Milton. The computation of OHC used 12 °C isotherm as the lower boundary. The section in (c) is used to plot the vertical profiles in Figure S7.

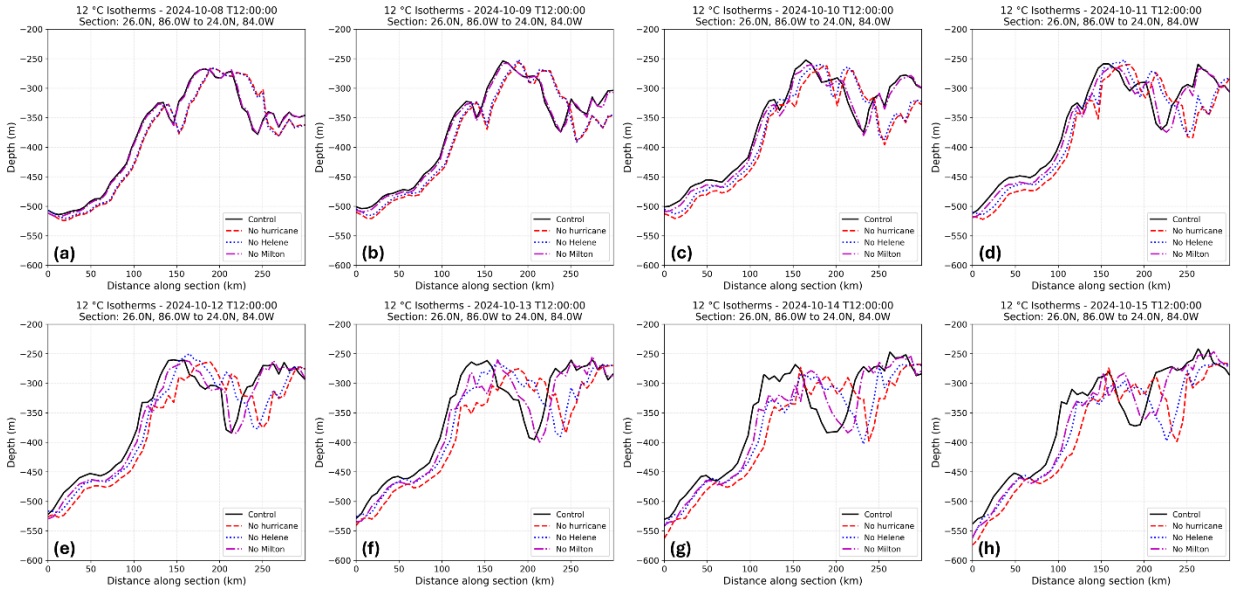

Figure S7. The 12°C isotherms and their depths for control and various hurricane-denial experiments from Oct 8th through 15th 2024. The location of the section is shown in Figure S6c.